Interpretation of NO_3-N_2O_5 observation via steady state in high aerosol air mass: The impact of equilibrium coefficient in ambient conditions

Xiaorui Chen[1], Haichao Wang[3,4], Keding Lu[1,2]

[1]State Key Joint Laboratory of Environmental Simulation and Pollution Control, College of Environmental Sciences and Engineering, Peking University, Beijing, China.

[2]The State Environmental Protection Key Laboratory of Atmospheric Ozone Pollution Control, College of Environmental Sciences and Engineering, Peking University, Beijing, China

[3]School of Atmospheric Sciences, Sun Yat-sen University, Zhuhai, 519082, China

[4]Guangdong Provincial Observation and Research Station for Climate Environment and Air Quality Change in the Pearl River Estuary, Key Laboratory of Tropical Atmosphere-Ocean System, Ministry of Education, Southern Marine Science and Engineering Guangdong Laboratory (Zhuhai), Zhuhai, 519082, China

Correspondence to: Haichao Wang (wanghch27@mail.sysu.edu.cn), Keding Lu (k.lu@pku.edu.cn)

Abstract. Steady state approximation for interpreting NO_3 and N_2O_5 has large uncertainty under complicated ambient conditions and could even produces incorrect results unconsciously. To provide an assessment and solution to the dilemma, we formulate data sets based on in-situ observations to reassess the applicability of the method. In most of steady state cases, we find a prominent discrepancy between *K*eq (equilibrium coefficient for reversible reactions of NO_3 and N_2O_5) and correspondingly simulated $[N_2O_5]/([NO_2]\times[NO_3])$, especially under high aerosol conditions in winter. This gap reveals the accuracy of *K*eq has a critical impact on the steady state analysis in polluted region. In addition, the accuracy of $\gamma(N_2O_5)$ derived by steady state fit depends closely on the reactivity of NO_3 (kNO_3) and N_2O_5 (kN_2O_5). Based on a complete set of simulations, air mass of kNO_3 less than 0.01 s^{-1} with high aerosol and temperature higher than 10°C is suggested to be the best suited for steady state analysis of NO_3-N_2O_5 chemistry. Instead of confirming the validity of steady state by numerical modeling for every case, this work directly provides appropriate concentration ranges for accurate steady state approximation, with implications for choosing suited methods to interpret nighttime chemistry in high aerosol air mass.

1 Introduction

Nitrate radical (NO_3), an extremely reactive species prone to build up at night, is an ideal candidate for steady state analysis in combine with dinitrogen pentoxide (N_2O_5) due to fast equilibrium reactions between them (R1).

$$NO_2 + NO_3 + M \rightarrow N_2O_5 + M \quad \text{(R1a)}$$

$$N_2O_5 + M \rightarrow NO_2 + NO_3 + M \quad \text{(R1b)}$$

Under the steady state condition, the lifetime of NO_3 (denoted as $\tau_{ss}(NO_3)$) can be calculated as the ratio of NO_3 concentration over the production rate ($k_{NO_2+O_3}[NO_2][O_3]$) or over the removal rate of both NO_3 and N_2O_5, as indicated in Eq. (1). A similar representation of N_2O_5 steady state lifetime is also shown in Eq. (2). The loss frequencies of various sink pathways of NO_3 and N_2O_5 are integrated as total first-order in the following equations, represented by kNO3 and kN2O5 term. Briefly, the kNO3 is contributed by the reaction of NO_3 radical with NO and hydrocarbons and uptake on particles at night, ranging from hundredths of s^{-1} to several s^{-1} depending on the air mass. Due to its large rate constant with NO, the concentration usually dominates the lifetime of NO_3 radical in urban areas with fresh NO emission. Otherwise, the reactions with hydrocarbons, especially unsaturated hydrocarbons, is preferential for NO_3 in rural areas. The Keq denotes the equilibrium coefficient for reactions R1a and R1b, used to be derived by Eq. (3).

$$\tau_{ss}(NO_3) \equiv \frac{[NO_3]}{k_{R1}[NO_2][O_3]} \approx (k_{NO_3} + K_{eq}[NO_2]k_{N_2O_5})^{-1}, \quad (1)$$

$$\tau_{ss}(N_2O_5) \equiv \frac{[N_2O_5]}{k_{R1}[NO_2][O_3]} \approx (k_{N_2O_5} + \frac{k_{NO_3}}{K_{eq}[NO_2]})^{-1}, \quad (2)$$

$$K_{eq} = \frac{k_{R1a}}{k_{R1b}} = \frac{[N_2O_5]}{[NO_2][NO_3]}, \quad (3)$$

Numerous works have taken the advantage of the steady state calculation to quantify the total first-order loss rate for NO_3 or N_2O_5 such that they drew conclusions about the oxidation capacity and reactive nitrogen budgets contributed by this chemical system (Allan et al., 1999;Allan et al., 2000;Carslaw et al., 1997;Platt et al., 1984;Vrekoussis et al., 2007;Wang et al., 2013). Since the steady state approximation was used to interpret atmospheric observation of NO_3-N_2O_5 (Brown, 2003; Platt et al., 1981), this method was also widely implemented to quantify N_2O_5 uptake coefficient ($\gamma(N_2O_5)$) (Brown et al., 2009;Brown et al., 2003;Li et al., 2020;McDuffie et al., 2019;Phillips et al., 2016;Wang et al., 2017a;Wang et al., 2017c;Wang et al., 2020a).

However, with the influence induced by complicated atmospheric conditions and emission, the steady state in ambient air mass will not always be the case (as illustrated in Text

S1 and Figure S1). These situations are prevalent in nocturnal boundary layer (Phillips et al., 2016;Stutz et al., 2004;Wang et al., 2017a;Wang et al., 2017c) and therefore increase the difficulty of applying steady state directly on NO_3-N_2O_5 observation data, whereas few studies have systematically characterized the error source and application conditions of this method (Brown et al., 2009).

Due to faster approach to equilibrium than steady state, the application of *K*eq in calculation steady state equations seems to be reasonable (Brown et al., 2003). For example, the ambient NO_3 concentration was usually calculated based on ambient N_2O_5 concentration with *K*eq×[NO_2] when determining their budgets or characterizing the lifetime or sink attribution of these two reactive nitrogen compounds (Brown et al., 2011;Osthoff et al., 2006;Wang et al., 2018;Wang et al., 2017c;Wang et al., 2017d;Yan et al., 2019). In addition, the mathematical conversion between NO_3 and N_2O_5 concentration via *K*eq coefficient can simplified the calculation in the iterative box model, which derives $\gamma(N_2O_5)$ by iterating its value in the model until the predicted N_2O_5 concentration matches the observation (Wagner et al., 2013;Wang et al., 2020b). However, considerable uncertainty could be associated with the quantification of *K*eq and its different parameterizations (Cantrell et al., 1988;Pritchard, 1994). The impact of *K*eq value on steady state fit or concentration conversion have not been explored to date in the analysis of NO_3-N_2O_5 steady state.

In this study, we formulate a half artificial dataset with expected properties based on field campaigns. Specifically, most of species contained in the dataset are observed values while only NO_3 and N_2O_5 were calculated by the steady state model (illustrated in the section 2.2). With the dataset, we illustrate the reasons for deviation of parameterized *K*eq from $[N_2O_5]/([NO_2]\times[NO_3])$ in ambient conditions, the possible uncertainties of linear fit based on steady state equations Eq. (4) and Eq. (5) (the related variables are explained in section 2.1) resulted from different *K*eq, and the influence of relevant atmospheric variables on $\gamma(N_2O_5)$ derivation via steady state method. Furthermore, a series of ambient condition tests specify the exact ranges suited for steady state analysis according to not only the validity of steady state but also *K*eq values, which optimizes the validity check by numerical modeling in previous research (Brown et al., 2009;Brown et al., 2003) and develops complete standard for data filtering.

2 Methods

2.1 γ(N_2O_5) derivation by steady state approximation

The framework of steady state approximation for NO_3-N_2O_5 system is basically built on its chemical production and removal pathways, in case of extremely weak physical processes (e.g. transport, dilution and deposition) relative to its chemical processes. With simultaneous measurements of NO_3, N_2O_5 and relevant precursor concentrations, the steady state lifetime $\tau_{ss}(NO_3)$ and $\tau_{ss}(N_2O_5)$ can be quantified for a targeted period as shown in Eq. (1) and Eq. (2). By substituting the $k$$N_2O_5$ with $0.25 \times c \times S_a \times \gamma(N_2O_5)$, the $\gamma(N_2O_5)$ and the reactivity of NO_3 ($k$$NO_3$, including the reactions of NO_3 with NO and hydrocarbons) can therefore be determined by Eq. (4) and Eq. (5).

$$\tau_{ss}{}^{-1}(\mathrm{NO_3}) \approx k_{NO_3} + \ 0.25 c S_a K_{eq}[\mathrm{NO_2}]\gamma(N_2O_5), \quad (4)$$

$$\left(0.25 c S_a \tau_{ss}(\mathrm{N_2O_5})\right)^{-1} \approx \ \gamma\,(N_2O_5) + \ k_{NO_3}\left(0.25 c S_a K_{eq}[\mathrm{NO_2}]\right)^{-1}, \quad (5)$$

Here c represents the mean molecular velocity of N_2O_5, Sa represents the aerosol surface area and the Keq is calculated from the rate constant of reversible reactions R1a (k_{R1a}) and R1b (k_{R1b}), which is a temperature-dependent parameter. It should be noted that the photolysis of NO_3 is not considered in the $k$$NO_3$ due to weak radiation at night and the homogeneous hydrolysis was also ignored due to its small contribution in comparison to heterogeneous pathway, similar presumption was also implemented in previous studies (Brown et al., 2009;Mentel et al., 1996;Wahner et al., 1998). In the form of these two equations, the potential covariance between Sa and NO_2 concentration can be avoided to decrease the uncertainty (Brown et al., 2009). By fit to these two equations, $\gamma(N_2O_5)$ can be directly derived from slope of the plot of $\tau_{ss}{}^{-1}(\mathrm{NO_3})$ against $0.25 c S_a K_{eq}[\mathrm{NO_2}]$ or from intercept of the plot of $\left(0.25 c S_a \tau_{ss}(\mathrm{N_2O_5})\right)^{-1}$ against $\left(0.25 c S_a K_{eq}[\mathrm{NO_2}]\right)^{-1}$ respectively. In the following analysis, the linear fit based on Eq. (5) is preferred in steady state approximation.

2.2 Steady state model and half-artificial datasets

The steady state model is reformed from 0-dimension box model to produce NO_3 and N_2O_5 which are in steady state as far as possible. It is constrained by measurements of NO, NO_2, O3, CO, CH_4, VOCs, HCHO, Sa, relative humidity (RH), temperature (T), pressure, coupled with Regional Atmospheric Chemistry Mechanism, version 2 (RACM2). Each data point is treated as an independent air mass, aging 10 hours and keeping input constraint unchanged. As NO_3-N_2O_5 chemistry, the interest of this work, usually shows marked impacts during the night, only the time periods with negligible photolysis frequency are under consideration. In

the standard simulation (herein referred as Mod0), the uptake coefficient of N_2O_5 is set to 0.02, as a reasonable value of literatures (Brown et al., 2006;Chen et al., 2020;McDuffie et al., 2018;Morgan et al., 2015;Phillips et al., 2016;Wagner et al., 2013;Wang et al., 2017c;Yu et al., 2020).

Two half-artificial datasets are derived from PKU2017 and TZ2018 field campaigns (see Text S2) based on steady state model for analysis in the following sections. The simulated NO_3 and N_2O_5 and other observed values used for the constraints of steady state model jointly formulate these half-artificial datasets. Specifically, the NO_3 and N_2O_5 concentration in this dataset are the output of the steady state model simulation, and guaranteed to be in steady state with respect to other observed precursors. To verify the steady state of NO_3 and N_2O_5 for each data point, we filtered the data set according to deviation between steady state lifetime of N_2O_5 ($\tau_{ss}(\mathrm{N_2O_5}) = \frac{[\mathrm{N_2O_5}]}{k_{\mathrm{R1}}[\mathrm{NO_2}][\mathrm{O_3}]}$) and calculated lifetime of N_2O_5 ($\tau_{calc}(\mathrm{N_2O_5}) = (k_{N_2O_5} + \frac{k_{NO_3}}{K_{eq}[\mathrm{NO_2}]})^{-1}$). If the deviation exceeds 10% for a data point, it will be excluded from the following analysis. We presume that if any data point outputted from the model is still out of steady state in terms of NO_3 and N_2O_5, the sink rate constant of air mass represented by this data point should be too weak for steady state analysis within a reasonable timescale. In addition, the data higher than 5 ppbv NO is filtered out in the following calculation, since the resulting large variation of kNO$_3$ can bias the linear fit even though the NO_3 and N_2O_5 approach the steady state rapidly under high NO (discussed in 3.2). The fraction of excluded data is less than 8%, which are expected to have little influence on our results. The calculated nighttime loss fraction accounted by NO_3 and N_2O_5 show large discrepancy (see Text. S3 and Figure S2) between these two half-artificial datasets, which provide us a good opportunity to investigate the impacting factors on steady state approximation across different conditions.

Rather than using observation data directly, a half-artificial dataset can provide larger amount of valid data for steady state analysis with known $\gamma(N_2O_5)$ value. Besides, this method avoids the impacts from steady state deviation, which helps to analyze the factors influencing $\gamma(N_2O_5)$ quantification via steady state approximation backwards from a known steady state condition.

3 Results and discussion

3.1 Varying equilibrium coefficient under steady state

The rates of NO_3-N_2O_5 reversible reactions are expected to be equal for the steady state case, so that the equilibrium coefficient Keq can be determined from either the rate constant ratio of R1a and R1b or the ratio of $[N_2O_5]/([NO_2]\times[NO_3])$. Although this approach is reasonable

under ideal conditions, the exactly same rates between reversible reactions and the following calculation based on *K*eq scaling are not so appropriate for ambient atmosphere where the removal pathway for NO_3-N_2O_5 are not negligible, especially under the high aerosol loading condition. The NO_3-N_2O_5 achieves steady state after 1.5-hours evolution, when concentration and rates remain constant (Figure 1). In this simulation, the starting mixing ratios of NO_2 and O_3 are 10 and 23 ppbv respectively, which is the average level for the nighttime conditions in PKU2017. The concentration of these two precursors are held constant in the simulation to better illustrate the influence of removal rates. This result will stay almost the same no matter these starting values are initialized to be constant or allowed to vary. Under steady state, the net equilibrium reaction rate in Figure 1(b)&(c) stays negative and positive for NO_3 and N_2O_5 respectively. Besides, the absolute values and difference of the forward and backward reaction rates remain unchanged after achieving steady state. This result is similar with a previous numerical calculation study (Brown et al., 2003), while the deviation between reversible reaction rates becomes larger in our case.

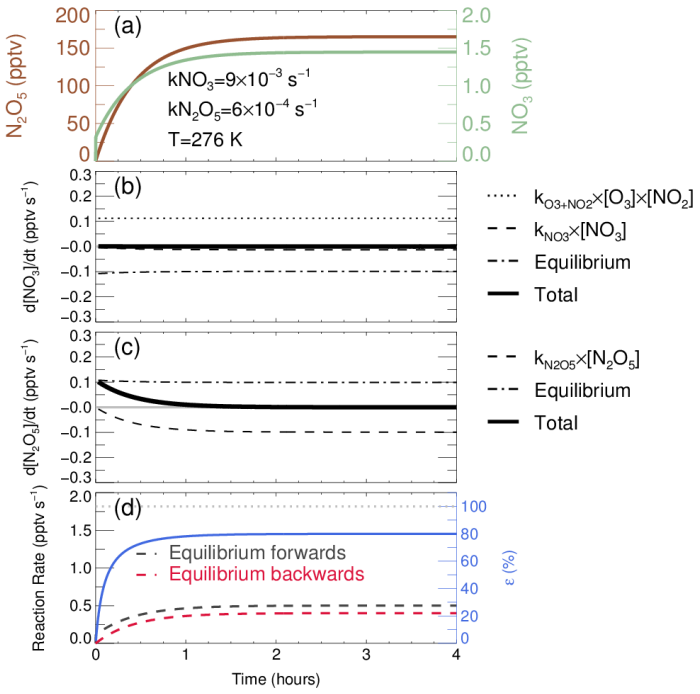

Figure 1. Evolution of NO_3-N_2O_5 system simulated by steady state model for an average case. (a) Temporal profiles of N_2O_5 and NO_3, the constraint of simulation is displayed as the text; (b) Evolution of d[NO_3]/dt calculated from source of $k_{O3+NO2}\times[O_3]\times[NO_2]$, sink of kNO$_3\times$[NO_3] and equilibrium terms, detailed in the text; (c) Evolution of d[N_2O_5]/dt calculated from equilibrium terms, sink of kN$_2$O$_5\times$[N_2O_5]; (d) Forward (N_2O_5 formation) and backward (N_2O_5 decomposition) equilibrium rate are represented as black and red dash lines, the equilibrium completeness ε is calculated by the ratio of backward rate over forward rate, shown as blue full line.

In this case, the original equilibrium is imperfect realized (a perfect realization of the original equilibrium condition is that *K*eq and the ratio of $[N_2O_5]/([NO_2] \times [NO_3])$ are equivalent as Eq. (6)), leading to errors on projection of NO_3 and N_2O_5 concentration via *K*eq $\times[NO_2]$. In fact, we note that a new equilibrium between NO_3 and N_2O_5 is developed with constant but unequal rates. Under this new equilibrium condition, the ratio of R1b reaction rate (the red dash line in Figure1(d)) over R1a reaction rate (the black dash line in Figure1(d)) can be regarded as the degree of approaching original equilibrium (the blue line in Figure1(d)). In addition, this value is also the ratio of $[N_2O_5]/([NO_2] \times [NO_3])$ against original *K*eq, therefore we defined this ratio as a correction factor ε, implemented to calculate accurate $[N_2O_5]/([NO_2] \times [NO_3])$ with significant N_2O_5 removal pathways. The value of *K*eq after scaled by ε can be used for converting the concentration of NO_3 and N_2O_5 via Eq. (6):

$$\varepsilon \times K_{eq} = \varepsilon \times \frac{k_{R1a}}{k_{R1b}} = \frac{[N_2O_5]}{[NO_2][NO_3]}, \quad (6)$$

Sensitivity tests are conducted to demonstrate the dependence of ε on relevant variables based on steady state model. The average ambient conditions observed at wintertime PKU site and summertime TZ site are taken as basic constraint for sensitivity tests (Table S2), respectively. By separately altering variables, such as NO_2, O_3, kN_2O_5, kNO_3 and T, the sensitivity of ε value can be obtained as shown in Figure 2 and Figure S4. The ε value depends primarily on kN_2O_5 and *T* in both scenarios, where ε increases with *T* (approaching 1 under relatively high *T*) and decreases with kN_2O_5. In comparison, the ε value behaves insensitive to kNO_3 as well as NO_2 and O_3 concentration, at least within the range of reasonable ambient conditions. High kN_2O_5 is resulted from high aerosol events, usually occur in winter accompanied with low temperature and high relative humidity in some populated areas (Baasandorj et al., 2017;Huang et al., 2014;Wang et al., 2017b;Wang et al., 2014), further decreasing the accuracy of original *K*eq values. It can be inferred that in order to accurately interpreting relationship of NO_3 and N_2O_5, calculation relying on equilibrium equation and steady state approximation should consider the dependence of ε on ambient conditions.

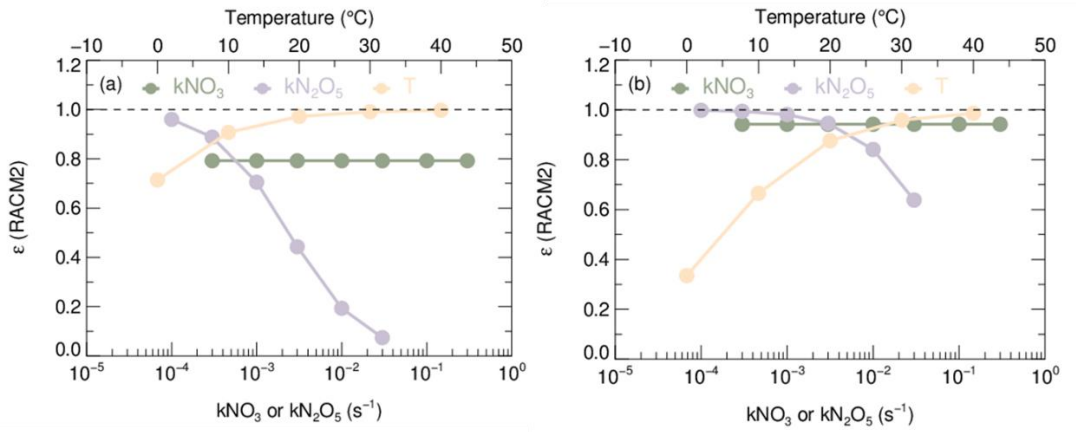

205

206 **Figure 2.** Sensitivity plot of $k\mathrm{NO_3}$, $k\mathrm{N_2O_5}$ and Temperature (T) against coefficient ε. The trace of T is
207 plotted against the upper horizontal axis and the traces of the other two parameters are plotted against the
208 lower horizontal axis. (a) Basic model condition is according to typical winter condition of PKU2017; (b)
209 Basic model condition is according to typical summer condition of TZ2018. Basic model conditions
210 including $k\mathrm{NO_3}$, $k\mathrm{N_2O_5}$ and Temperature (T) are shown in Table S2. It should be noted that the provided
211 ranges of each factor do not exactly equal to but encompass the ambient conditions encountered during the
212 two campaigns.

213 Even if *K*eq value serves as a good representation of the ratio of $[\mathrm{N_2O_5}]/([\mathrm{NO_2}]\times[\mathrm{NO_3}])$
214 or ε can be readily quantified on field, the discrepancy among different database in
215 calculating *K*eq still increase the uncertainties of $\mathrm{NO_3}$-$\mathrm{N_2O_5}$ calculation through steady state
216 approximation or equilibrium, which has not been carefully considered. Here, we apply a set
217 of uniform formulas to describing k_{R1a} and k_{R1b} (see Text. S4) from preferred values of several
218 popular atmospheric chemistry mechanisms (Mozart, CB05, Saprc07, RACM2 and kinetic
219 databases JPL2015 as well as IUPAC2017) and finally calculating *K*eq. As is shown in Figure
220 S5 and Figure S6, *K*eq variations derived from these six different databases reflect
221 considerable discrepancy from each other, especially in colder conditions. Because
222 parameterized *K*eq values are only dependent on ambient temperature, they continuously
223 increase with time due to the decrease of temperature. In addition to discrepancy between
224 different *K*eq parameterizations, ε value varies dissimilarly with each *K*eq, ranging from 70%
225 to 90%. All these results demonstrate that, in most cases, *K*eq values simply derived from
226 existing database would fail to reproduce accurate relationship between $\mathrm{NO_3}$ and $\mathrm{N_2O_5}$.

227 To further elucidate the impact of *K*eq on deriving $\gamma(\mathrm{N_2O_5})$ via steady state approximation
228 (hereafter defined as $\gamma_{ss}(\mathrm{N_2O_5})$), Figure S6 shows the steady state fit based on all six database-
229 derived *K*eq and in the same time periods as Figure S5 through Eq. (4) and Eq. (5) respectively
230 (both of equations can derive a pair of $\gamma_{ss}(\mathrm{N_2O_5})$ and $k\mathrm{NO_3}$). The *K*eq (corrected with ε) is
231 calculated with $\mathrm{NO_3}$ and $\mathrm{N_2O_5}$ concentration simulated based on RACM2. Fit based on Eq. (4)

could lead to 11~46% underestimation of $\gamma_{ss}(N_2O_5)$, as indicated by varying slopes in Figure S7(b)&(d), when using the database-derived *K*eq. Conversely, fit by Eq. (5) (shown in Figure S7(a)&(c)) bias the result of kNO$_3$ served as the slopes without much influence on $\gamma_{ss}(N_2O_5)$ served as the intercept. Previous research ascribed inconsistent fit results between two equations to measurements uncertainty (Brown et al., 2009;Brown et al., 2006). However, fit with original *K*eq might be the primary reasons for such inconsistent results, and even deviates the derived $\gamma_{ss}(N_2O_5)$ and kNO$_3$ from true values. Therefore, steady state fit based on Eq. (5) might be the best choice for $\gamma(N_2O_5)$ derivation via steady state approximation. Similarly, Eq. (4) is preferred to be applied when kNO$_3$ is the final objective.

3.2 Impacts of NO_3-N_2O_5 reactivity on steady state

In order to further explore the impacting factors on steady state fit method, $\gamma_{ss}(N_2O_5)$ results are derived for each 2-hour time period of PKU2017 and TZ2018 dataset based on output from steady state model. Since the pre-set $\gamma(N_2O_5)$ in this model is 0.02, the degree of deviation from this value is supposed to reflect the accuracy of the fitted result.

It can be noticed from Eq. (5) that the variability of kNO$_3$ during the same time period leads data points to scatter on lines with different slopes, which could bias the resulted $\gamma_{ss}(N_2O_5)$ from model pre-set value. As is shown in Figure 3, the absolute percentages of $\gamma_{ss}(N_2O_5)$ deviation grow dramatically with the increase of relative standard deviation of kNO$_3$ (kNO$_3$ RSD) in both of winter and summer data sets. The positive correlation even gives rise to extreme deviation in summer data set with up to almost 10 times of model setting $\gamma(N_2O_5)$. In fact, there remains accurate $\gamma_{ss}(N_2O_5)$ values derived in each range of kNO$_3$ RSD, indicating a not strictly positive correlation between $\gamma_{ss}(N_2O_5)$ deviation and kNO$_3$ RSD. It implies that large variation of kNO$_3$ only enhance the possibilities of inaccurate results from steady state fit rather than hinder the $\gamma_{ss}(N_2O_5)$ quantification all the time.

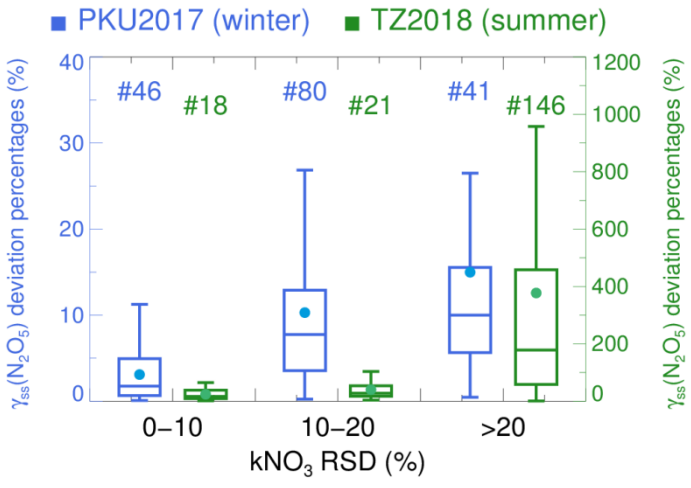

Figure 3. Relationship between $\gamma(N_2O_5)$ derivation through steady state approximation and kNO$_3$ relative standard deviation (RSD) in box whisker plot. The blue and green color represent dataset from PKU2017 and TZ2018 respectively, binned according to kNO$_3$ RSD. The dots are the mean deviation of $\gamma_{ss}(N_2O_5)$. The number above the box whisker represents the valid data points in each bin.

Besides the large variation of kNO$_3$ in short time period, the absolute level of kNO$_3$ and kN$_2$O$_5$ could influence the possibilities of inaccurate $\gamma_{ss}(N_2O_5)$ from different aspects. Although the enhancement of kNO$_3$ and kN$_2$O$_5$ boost the approach to steady state (Text. S5 and Figure S8), higher levels of kNO$_3$ amplify the bias of $\gamma_{ss}(N_2O_5)$, contrary to kN$_2$O$_5$, with the same relative variation of kNO$_3$ (Text. S6 and Figure S10). It indicates that the region with plural emissions (e.g. strong biogenic or vehicular emission) might not be suited for steady state fit due to the high kNO$_3$. Therefore, a trade-off between the variation of kNO$_3$ and the high level of kNO$_3$ (fast approach to steady state) should be made when derive $\gamma_{ss}(N_2O_5)$.

3.3 Implication for accurate steady state analysis of NO$_3$-N$_2$O$_5$

While a few studies have examined the validity of steady state under certain conditions via numerical modeling when interpreted the ambient data (Brown et al., 2009;Brown et al., 2003), a clear range well suited to steady state analysis of NO$_3$-N$_2$O$_5$, taking both Keq and validity of steady state into consideration, has not been determined to date.

Here almost 20000 simulations are displayed in the parallel plot of Figure 4, where each line connects 5 constraint parameters to the calculated steady state time and ε (the correction factor for Keq parameterization to match the exact ratio of $[N_2O_5]/([NO_2]\times[NO_3])$, detailed in Eq.6). The gray traces represent the simulations could not match steady state within 600 s and were defined as less valid cases here. By this definition, we intend to indicate that it is also viable to apply steady state approximation on air mass, which requires more than 600 s to match steady state, whereas the uncertainty caused therefrom could increase to some extent. The pink and blue traces together represent the simulations could match valid steady state within 600 s without consideration of Keq deviation (in other word the value of ε). Furthermore, the criterion to apply steady state approximation appropriately we defined is that approach to steady state within 600 s and the ε larger than 0.9, which are indicated as pink traces. While the level of T, NO$_2$ and O$_3$ have minor effect on the approach to steady state, simultaneous low kN$_2$O$_5$ (indicated as low Sa in the plot) and kNO$_3$ prevent the NO$_3$-N$_2$O$_5$ system from developing steady state. For example, when kNO$_3$ is lower than 0.01 s^{-1}, the air mass will be valid only if Sa increases to at least 3000 μm^2 cm^{-3} with $\gamma(N_2O_5)$ of 0.02. It implies that clean air mass is not suited for steady state in any cases, whereas high aerosol condition provides more possibilities to approach steady state even with low kNO$_3$. However, in order

to interpreting NO_3-N_2O_5 chemistry with accurate *K*eq coefficient, the ε larger than 0.9 is additionally taken into consideration, which excludes 50% of valid steady state cases mainly with high aerosol and lower than 10℃. These cases could bias $[N_2O_5]/([NO_2]\times[NO_3])$ from original *K*eq (also indicated in Figure 2), leading to inaccurate results of calculation based on *K*eq.

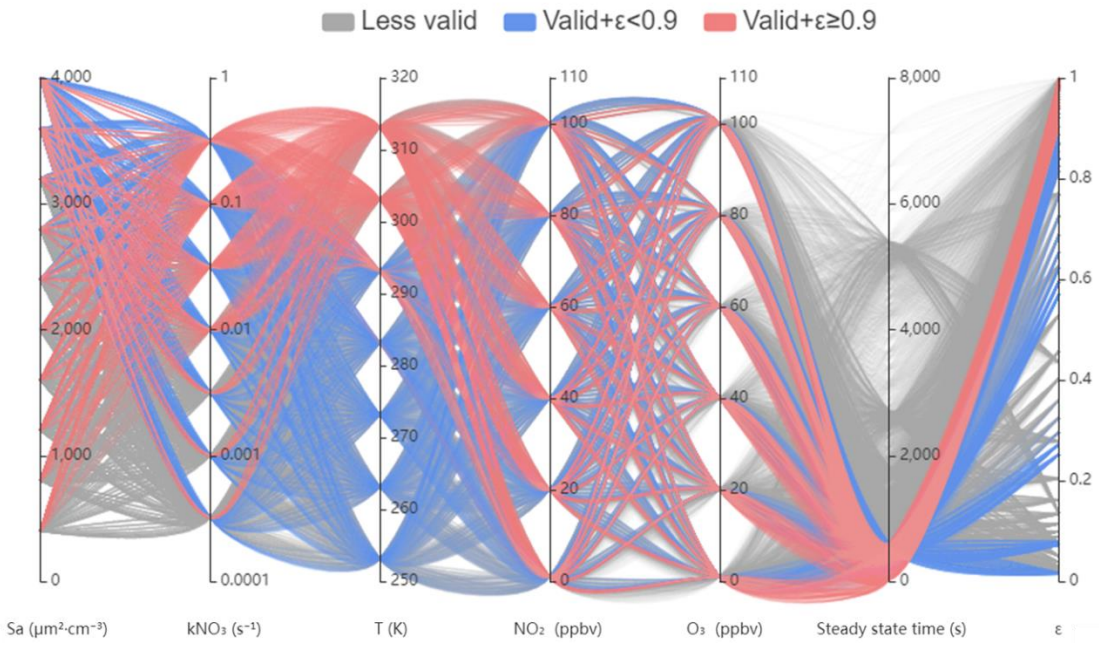

Figure 4. Numerical simulations for determining conditions available for steady state approximation method in a parallel axis plot. Each line simply represents a simulation associated with different parameters in different vertical axes. The first five axes from the left represent initial variables used for constraining the simulations respectively. The last two axes represent the time required for achieving steady state and the ε value calculated from the simulated results. The gray lines show cases approaching steady state longer than 600 s (less valid). The blue lines show cases approaching steady state cases within 600 s while with ε less than 0.9, which is also inappropriate for steady state analysis. The pink lines show cases approaching steady state cases within 600 s with ε higher than 0.9, which is suited for steady state analysis.

4 Conclusions

In this study, we found that the parameterized *K*eq coefficient deviates much from the ratio of $[N_2O_5]/([NO_2]\times[NO_3])$ in some cases where steady state is valid. The indicator of the deviation, ε, is relatively sensitive to N_2O_5 reactivity and ambient temperature. It implies that conditions suited for steady state analysis should be determined according to not only the validity of steady state but also *K*eq especially under high aerosol conditions, like some regions in India, China, Europe and the US (Baasandorj et al., 2017;Cesari et al., 2018;Huang et al., 2014;Mogno et al., 2021;Petit et al., 2017;Wang et al., 2017b). Considering that high level of

$k\mathrm{NO_3}$ might amplify the bias of $\gamma_{ss}(\mathrm{N_2O_5})$ yield from steady state fit and appears to be accompanied with fast variations, air mass of $k\mathrm{NO_3}$ less than 0.01 s^{-1} with high aerosol and T higher than 10℃ is therefore the best suited for steady state analysis of $\mathrm{NO_3}$-$\mathrm{N_2O_5}$ chemistry, which indicates that this method would be more applicable in polluted regions with high aerosol loading during summertime. If the restriction of ε is relaxed to 30%, some of winter conditions will also be applicable. Our results provide an insight to improve the accuracy of steady state approximation method and find suited areas to interpret nighttime chemistry. Further improvement of in-situ $\mathrm{NO_3}$-$\mathrm{N_2O_5}$ budgets quantification might relies on the direct measurements via flow tube system or machine learning prediction based on ancillary parameters.

Supporting Information: The Supporting Information is available on line.

Code/Data availability. The datasets used in this study are available from the corresponding author upon request (wanghch27@mail.sysu.edu.cn; k.lu@pku.edu.cn).

Author contributions. K.D.L. and H.C.W. designed the study. X.R.C and H.C.W. analyzed the data and wrote the paper with input from K.D.L.

Competing interests. The authors declare that they have no conflicts of interest.

Acknowledgments. This project is supported by the National Natural Science Foundation of China (21976006, 42175111); the Beijing Municipal Natural Science Foundation for Distinguished Young Scholars (JQ19031); National State Environmental Protection Key Laboratory of Formation and Prevention of Urban Air Pollution Complex (CX2020080578); the special fund of the State Key Joint Laboratory of Environment Simulation and Pollution Control (21K02ESPCP); the National Research Program for Key Issue in Air Pollution Control (DQGG0103-01, 2019YFC0214800). Thanks for the data contributed by field campaign team.

References

Allan, B. J., Carslaw, N., Coe, H., Burgess, R. A., and Plane, J. M. C.: Observations of the nitrate radical in the marine boundary layer, Journal of Atmospheric Chemistry, 33, 129-154, Doi 10.1023/A:1005917203307, 1999.

Allan, B. J., McFiggans, G., Plane, J. M. C., Coe, H., and McFadyen, G. G.: The nitrate radical in the remote

marine boundary layer, J. Geophys. Res.: Atmos., 105, 24191-24204, 10.1029/2000JD900314, 2000.
Baasandorj, M., Hoch, S. W., Bares, R., Lin, J. C., Brown, S. S., Millet, D. B., Martin, R., Kelly, K., Zarzana, K. J., Whiteman, C. D., Dube, W. P., Tonnesen, G., Jaramillo, I. C., and Sohl, J.: Coupling between Chemical and Meteorological Processes under Persistent Cold-Air Pool Conditions: Evolution of Wintertime PM2.5 Pollution Events and N2O5 Observations in Utah's Salt Lake Valley, Environmental Science & Technology, 51, 5941-5950, 10.1021/acs.est.6b06603, 2017.
Brown, S. S.: Applicability of the steady state approximation to the interpretation of atmospheric observations of NO3and N2O5, J. Geophys. Res. , 108, 10.1029/2003jd003407, 2003.
Brown, S. S., Stark, H., and Ravishankara, A. R.: Applicability of the steady state approximation to the interpretation of atmospheric observations of NO3 and N2O5, Journal of Geophysical Research-Atmospheres, 108, Artn 4539
Doi 10.1029/2003jd003407, 2003.
Brown, S. S., Ryerson, T. B., Wollny, A. G., Brock, C. A., Peltier, R., Sullivan, A. P., Weber, R. J., Dube, W. P., Trainer, M., Meagher, J. F., Fehsenfeld, F. C., and Ravishankara, A. R.: Variability in nocturnal nitrogen oxide processing and its role in regional air quality, Science, 311, 67-70, DOI 10.1126/science.1120120, 2006.
Brown, S. S., Dube, W. P., Fuchs, H., Ryerson, T. B., Wollny, A. G., Brock, C. A., Bahreini, R., Middlebrook, A. M., Neuman, J. A., Atlas, E., Roberts, J. M., Osthoff, H. D., Trainer, M., Fehsenfeld, F. C., and Ravishankara, A. R.: Reactive uptake coefficients for N2O5 determined from aircraft measurements during the Second Texas Air Quality Study: Comparison to current model parameterizations, J. Geophys. Res.- Atmos., 114, D00F10(01-16), Artn D00f10
10.1029/2008jd011679, 2009.
Brown, S. S., Dubé, W. P., Peischl, J., Ryerson, T. B., Atlas, E., Warneke, C., de Gouw, J. A., te Lintel Hekkert, S., Brock, C. A., Flocke, F., Trainer, M., Parrish, D. D., Feshenfeld, F. C., and Ravishankara, A. R.: Budgets for nocturnal VOC oxidation by nitrate radicals aloft during the 2006 Texas Air Quality Study, J. Geophys. Res.: Atmos., 116, 10.1029/2011jd016544, 2011.
Cantrell, C., Davidson, J., McDaniel, A., Shetter, R., and Calvert, J.: The equilibrium constant for N2O5 = NO2 + NO3 - Absolute determination by direct measurement from 243 to 397 K, The Journal of Chemical Physics, 88, 10.1063/1.454679, 1988.
Carslaw, N., Plane, J. M. C., Coe, H., and Cuevas, E.: Observations of the nitrate radical in the free troposphere at Izana de Tenerife, J. Geophys. Res.- Atmos., 102, 10613-10622, 10.1029/96jd03512, 1997.
Cesari, D., De Benedetto, G. E., Bonasoni, P., Busetto, M., Dinoi, A., Merico, E., Chirizzi, D., Cristofanelli, P., Donateo, A., Grasso, F. M., Marinoni, A., Pennetta, A., and Contini, D.: Seasonal variability of PM2.5 and PM10 composition and sources in an urban background site in Southern Italy, Science of the Total Environment, 612, 202-213, 10.1016/j.scitotenv.2017.08.230, 2018.
Chen, X., Wang, H., Lu, K., Li, C., Zhai, T., Tan, Z., Ma, X., Yang, X., Liu, Y., Chen, S., Dong, H., Li, X., Wu, Z., Hu, M., Zeng, L., and Zhang, Y.: Field Determination of Nitrate Formation Pathway in Winter Beijing, Environmental Science & Technology, 54, 9243-9253, 10.1021/acs.est.0c00972, 2020.
Huang, R.-J., Zhang, Y., Bozzetti, C., Ho, K.-F., Cao, J.-J., Han, Y., Daellenbach, K. R., Slowik, J. G., Platt, S. M., Canonaco, F., Zotter, P., Wolf, R., Pieber, S. M., Bruns, E. A., Crippa, M., Ciarelli, G., Piazzalunga, A., Schwikowski, M., Abbaszade, G., Schnelle-Kreis, J., Zimmermann, R., An, Z., Szidat, S., Baltensperger, U., Haddad, I. E., and Prévôt, A. S. H.: High secondary aerosol contribution to particulate pollution during haze events in China, Nature, 514, 218-222, 10.1038/nature13774, 2014.

Li, Z. Y., Xie, P. H., Hu, R. Z., Wang, D., Jin, H. W., Chen, H., Lin, C., and Liu, W. Q.: Observations of N2O5 and NO3 at a suburban environment in Yangtze river delta in China: Estimating heterogeneous N2O5 uptake coefficients, J. Environ. Sci., 95, 248-255, 10.1016/j.jes.2020.04.041, 2020.

McDuffie, E. E., Fibiger, D. L., Dubé, W. P., Lopez-Hilfiker, F., Lee, B. H., Thornton, J. A., Shah, V., Jaeglé, L., Guo, H., Weber, R. J., Michael Reeves, J., Weinheimer, A. J., Schroder, J. C., Campuzano-Jost, P., Jimenez, J. L., Dibb, J. E., Veres, P., Ebben, C., Sparks, T. L., Wooldridge, P. J., Cohen, R. C., Hornbrook, R. S., Apel, E. C., Campos, T., Hall, S. R., Ullmann, K., and Brown, S. S.: Heterogeneous N_2O_5 Uptake During Winter: Aircraft Measurements During the 2015 WINTER Campaign and Critical Evaluation of Current Parameterizations, J. Geophys. Res.: Atmos., 123, 4345-4372, 10.1002/2018jd028336, 2018.

McDuffie, E. E., Womack, C. C., Fibiger, D. L., Dube, W. P., Franchin, A., Middlebrook, A. M., Goldberger, L., Lee, B. H., Thornton, J. A., Moravek, A., Murphy, J. G., Baasandorj, M., and Brown, S. S.: On the contribution of nocturnal heterogeneous reactive nitrogen chemistry to particulate matter formation during wintertime pollution events in Northern Utah, Atmos. Chem. Phys., 19, 9287-9308, 10.5194/acp-19-9287-2019, 2019.

Mentel, T. F., Bleilebens, D., and Wahner, A.: A study of nighttime nitrogen oxide oxidation in a large reaction chamber - The fate of NO2 N2O5, HNO3, and O-3 at different humidities, Atmos. Environ., 30, 4007-4020, 10.1016/1352-2310(96)00117-3, 1996.

Mogno, C., Palmer, P. I., Knote, C., Yao, F., and Wallington, T. J.: Seasonal distribution and drivers of surface fine particulate matter and organic aerosol over the Indo-Gangetic Plain, Atmos. Chem. Phys., 21, 10881-10909, 10.5194/acp-21-10881-2021, 2021.

Morgan, W. T., Ouyang, B., Allan, J. D., Aruffo, E., Di Carlo, P., Kennedy, O. J., Lowe, D., Flynn, M. J., Rosenberg, P. D., Williams, P. I., Jones, R., McFiggans, G. B., and Coe, H.: Influence of aerosol chemical composition on N2O5 uptake: airborne regional measurements in northwestern Europe, Atmospheric Chemistry and Physics, 15, 973-990, DOI 10.5194/acp-15-973-2015, 2015.

Osthoff, H. D., Sommariva, R., Baynard, T., Pettersson, A., Williams, E. J., Lerner, B. M., Roberts, J. M., Stark, H., Goldan, P. D., Kuster, W. C., Bates, T. S., Coffman, D., Ravishankara, A. R., and Brown, S. S.: Observation of daytime N2O5 in the marine boundary layer during New England Air Quality Study - Intercontinental Transport and Chemical Transformation 2004, Journal of Geophysical Research-Atmospheres, 111, Artn D23s14 10.1029/2006jd007593, 2006.

Petit, J. E., Amodeo, T., Meleux, F., Bessagnet, B., Menut, L., Grenier, D., Pellan, Y., Ockler, A., Rocq, B., Gros, V., Sciare, J., and Favez, O.: Characterising an intense PM pollution episode in March 2015 in France from multi-site approach and near real time data: Climatology, variabilities, geographical origins and model evaluation, Atmospheric Environment, 155, 68-84, 10.1016/j.atmosenv.2017.02.012, 2017.

Phillips, G. J., Thieser, J., Tang, M., Sobanski, N., Schuster, G., Fachinger, J., Drewnick, F., Borrmann, S., Bingemer, H., Lelieveld, J., and Crowley, J. N.: Estimating N_2O_5 uptake coefficients using ambient measurements of NO_3, N_2O_5, $ClNO_2$ and particle-phase nitrate, Atmos. Chem. Phys., 16, 13231-13249, 10.5194/acp-16-13231-2016, 2016.

Platt, U., Perner, D., Schroder, J., Kessler, C., and Toennissen, A.: The Diurnal-Variation of NO3, J Geophys Res-Oceans, 86, 1965-1970, DOI 10.1029/JC086iC12p11965, 1981.

Platt, U. F., Winer, A. M., Biermann, H. W., Atkinson, R., and Pitts, J. N.: Measurement of nitrate radical concentrations in continental air, Environmental Science & Technology, 18, 365-369, 10.1021/es00123a015, 1984.

Pritchard, H.: The nitrogen pentoxide dissociation equilibrium, Int. J. Chem. Kinet., 26, 61-71,

10.1002/kin.550260108, 1994.
Stutz, J., Alicke, B., Ackermann, R., Geyer, A., White, A., and Williams, E.: Vertical profiles of NO3, N2O5, O-3, and NOx in the nocturnal boundary layer: 1. Observations during the Texas Air Quality Study 2000, J. Geophys. Res.- Atmos., 109, 10.1029/2003jd004209, 2004.
Vrekoussis, M., Mihalopoulos, N., Gerasopoulos, E., Kanakidou, M., Crutzen, P. J., and Lelieveld, J.: Two-years of NO3 radical observations in the boundary layer over the Eastern Mediterranean, Atmospheric Chemistry and Physics, 7, 315-327, 2007.
Wagner, N. L., Riedel, T. P., Young, C. J., Bahreini, R., Brock, C. A., Dubé, W. P., Kim, S., Middlebrook, A. M., Öztürk, F., Roberts, J. M., Russo, R., Sive, B., Swarthout, R., Thornton, J. A., VandenBoer, T. C., Zhou, Y., and Brown, S. S.: N2O5 uptake coefficients and nocturnal NO2 removal rates determined from ambient wintertime measurements, J. Geophys. Res.: Atmos., 118, 9331-9350, 10.1002/jgrd.50653, 2013.
Wahner, A., Mentel, T. F., Sohn, M., and Stier, J.: Heterogeneous reaction of N2O5 on sodium nitrate aerosol, J. Geophys. Res.: Atmos., 103, 31103-31112, 10.1029/1998jd100022, 1998.
Wang, H., Lu, K., Chen, X., Zhu, Q., Chen, Q., Guo, S., Jiang, M., Li, X., Shang, D., Tan, Z., Wu, Y., Wu, Z., Zou, Q., Zheng, Y., Zeng, L., Zhu, T., Hu, M., and Zhang, Y.: High N_2O_5 Concentrations Observed in Urban Beijing: Implications of a Large Nitrate Formation Pathway, Environ Sci Tech Let, 4, 416-420, 10.1021/acs.estlett.7b00341, 2017a.
Wang, H., Chen, X., Lu, K., Hu, R., Li, Z., Wang, H., Ma, X., Yang, X., Chen, S., Dong, H., Liu, Y., Fang, X., Zeng, L., Hu, M., and Zhang, Y.: NO3 and N2O5 chemistry at a suburban site during the EXPLORE-YRD campaign in 2018, Atmospheric Environment, 224, 10.1016/j.atmosenv.2019.117180, 2020a.
Wang, H., Chen, X., Lu, K., Tan, Z., Ma, X., Wu, Z., Li, X., Liu, Y., Shang, D., Wu, Y., Zeng, L., Hu, M., Schmitt, S., Kiendler-Scharr, A., Wahner, A., and Zhang, Y.: Wintertime N2O5 uptake coefficients over the North China Plain, Science Bulletin, 65, 765-774, 10.1016/j.scib.2020.02.006, 2020b.
Wang, H. C., Lu, K. D., Guo, S., Wu, Z. J., Shang, D. J., Tan, Z. F., Wang, Y. J., Le Breton, M., Lou, S. R., Tang, M. J., Wu, Y. S., Zhu, W. F., Zheng, J., Zeng, L. M., Hallquist, M., Hu, M., and Zhang, Y. H.: Efficient N2O5 uptake and NO3 oxidation in the outflow of urban Beijing, Atmos. Chem. Phys., 18, 9705-9721, 10.5194/acp-18-9705-2018, 2018.
Wang, J., Zhao, B., Wang, S., Yang, F., Xing, J., Morawska, L., Ding, A., Kulmala, M., Kerminen, V.-M., Kujansuu, J., Wang, Z., Ding, D., Zhang, X., Wang, H., Tian, M., Petäjä, T., Jiang, J., and Hao, J.: Particulate matter pollution over China and the effects of control policies, Sci. Total Environ., 584-585, 426-447, https://doi.org/10.1016/j.scitotenv.2017.01.027, 2017b.
Wang, S., Shi, C., Zhou, B., Zhao, H., Wang, Z., Yang, S., and Chen, L.: Observation of NO3 radicals over Shanghai, China, Atmos. Environ., 70, 401-409, 10.1016/j.atmosenv.2013.01.022, 2013.
Wang, X., Wang, H., Xue, L., Wang, T., Wang, L., Gu, R., Wang, W., Tham, Y. J., Wang, Z., Yang, L., Chen, J., and Wang, W.: Observations of N_2O_5 and $ClNO_2$ at a polluted urban surface site in North China: High N_2O_5 uptake coefficients and low $ClNO_2$ product yields, Atmos. Environ., 156, 125-134, 10.1016/j.atmosenv.2017.02.035, 2017c.
Wang, Y., Yao, L., Wang, L., Liu, Z., Ji, D., Tang, G., Zhang, J., Sun, Y., Hu, B., and Xin, J.: Mechanism for the formation of the January 2013 heavy haze pollution episode over central and eastern China, Science China Earth Sciences, 57, 14-25, 10.1007/s11430-013-4773-4, 2014.
Wang, Z., Wang, W., Tham, Y. J., Li, Q., Wang, H., Wen, L., Wang, X., and Wang, T.: Fast heterogeneous N2O5 uptake and ClNO2 production in power plant and industrial plumes observed in the nocturnal residual layer over

the North China Plain, Atmos. Chem. Phys., 17, 12361-12378, 10.5194/acp-17-12361-2017, 2017d.
Yan, C., Tham, Y. J., Zha, Q. Z., Wang, X. F., Xue, L. K., Dai, J. N., Wang, Z., and Wang, T.: Fast heterogeneous loss of N2O5 leads to significant nighttime NOx removal and nitrate aerosol formation at a coastal background environment of southern China, Science of the Total Environment, 677, 637-647, 10.1016/j.scitotenv.2019.04.389, 2019.
Yu, C., Wang, Z., Xia, M., Fu, X., Wang, W., Yee Jun, T., Chen, T., Zheng, P., Li, H., Shan, Y., Wang, X., Xue, L., Zhou, Y., Yue, D., Ou, Y., Gao, J., Lu, K., Brown, S., Zhang, Y., and Tao, W.: Heterogeneous N_2O_5 reactions on atmospheric aerosols at four Chinese sites: improving model representation of uptake parameters, Atmos. Chem. Phys., 20, 4367-4378, 10.5194/acp-20-4367-2020, 2020.